

On Fast SC-based Polar Decoders: Metric Polarization and a Pruning Technique

Mohsen Moradi¹, Hessam Mahdavi¹

Abstract—Short- to medium-block-length polar-like and polarization-adjusted convolutional (PAC) codes have demonstrated exceptional error-correction performance through sequential decoding. Successive cancellation list (SCL) decoding of polar-like and PAC codes can potentially match the performance of sequential decoding though a relatively large list size is often required. By benefiting from an optimal metric function, sequential decoding can find the correct path corresponding to the transmitted data by following almost one path on average at high E_b/N_0 regimes. When considering a large number of paths in SCL decoding, a main bottleneck emerges that is the need for a rather expensive sorting operation at each level of decoding of data bits. In this paper, we propose a method to obtain the optimal metric function for each depth of the polarization tree through a process that we call *polarization* of the metric function. One of the major advantages of the proposed metric function is that it can be utilized in *fast* SC-based (FSC) and SCL-based (FSCL) decoders, i.e., decoders that opt to skip the so-called rate-1 and rate-0 nodes in the binary tree representation for significantly more efficient implementation. Furthermore, based on the average value of the polarized metric function of FSC-based decoders, we introduce a pruning technique that keeps only the paths whose metric values are close to the average value. As a result, our proposed technique significantly reduces the number of required sorting operations for FSCL-based decoding algorithms. For instance, for a high-rate PAC(128, 99) code, SCL decoding with a list size of 32 achieves error-correction performance comparable to the Fano algorithm. FSCL decoding requires visiting only 28 nodes of the polarization tree, significantly fewer than the 254 nodes required for conventional SCL decoding. Additionally, our method reduces the number of sorting operations to 33%, further decreasing latency.

Index Terms—PAC codes, SCL decoding, Fast SCL, polar coding, channel coding, polarization, optimal metric.

I. INTRODUCTION

THE rapid expansion of Internet of Things (IoT) applications and connected devices underscores the need for ultra-reliable, low-latency communication. Polar codes, introduced by Arikan [1], represent the first class of codes proven to achieve the capacity of memoryless symmetric channels with explicit constructions and low-complexity encoding and decoding. As an improvement to polar codes, polarization-adjusted convolutional (PAC) codes [2] are a new class of linear codes that demonstrate error-correction performance close to theoretical bounds in the short block-length regime [2], [3]. The main new ingredient of PAC codes is the use of convolutional codes as a pre-transformation that improves

upon the weight spectrum of polar codes [4]. PAC codes are also equivalent to post-transforming polar codes with certain cyclic codes [5].

PAC codes can be decoded using the Fano algorithm [6]. The Fano algorithm is a sequential decoding method that follows a single path on the decoding tree while accumulating a certain metric function. If a few consecutive information bits are decoded incorrectly, the value of the metric function typically drops, causing the algorithm to backtrack to the previously decoded bits and choose an alternative path. This process requires a metric function capable of comparing paths of different lengths optimally, which can be achieved by incorporating a bias value [7]. Fano-type decoders typically have a varying complexity, which can also become exponentially expensive [8]. This is not appealing from a hardware implementation perspective, where a certain budget on various parameters including latency and power consumption need to be assumed.

The successive cancellation list (SCL) decoding of polar codes [9] is also adapted for decoding PAC codes [10], [11]. To consider multiple paths simultaneously, SCL decoding with a list of size L evaluates $2L$ branches corresponding to each information bit and selects the best L branches based on a metric. Consequently, it follows up to L different paths on the decoding tree simultaneously. This approach requires an increase in the memory size by a factor of L compared to successive cancellation (SC) or Fano decoding. Further, to achieve a performance similar to that of the Fano algorithm, a relatively large list size is required. Hence, efforts to simplify the decoder in order to reduce its complexity and latency become desirable. In particular, deployment of *fast* SC (FSC) and SCL (FSCL) decoders, i.e., decoders that opt to skip the so-called rate-1 and rate-0 nodes in the binary tree representation for significantly more efficient implementation, are highly beneficial [12], [13].

In this paper, we introduce a method to derive the optimal metric function for each level of the polarization tree, a process we refer to as the *polarization* of the metric function. We demonstrate that, on average, the values of the metric functions at each level of the polarization tree correspond to the polarized mutual information for the correct branch and a negative value for the incorrect branch. A major advantage of the proposed metric function is that it can be utilized in FSC and FSCL decoders. In particular, the new method enables us to estimate the path metrics of fast SC-based decoders (fast SCL and fast Fano) that operate at the intermediate levels of the polarization tree. Simulation results show that our proposed average metric values perfectly match the path metric sample

The authors are with the Department of Electrical & Computer Engineering, Northeastern University, Boston MA-02115, USA (e-mail: m.moradi@northeastern.edu, h.mahdavi@northeastern.edu).

This work was supported by NSF under Grant CCF-2415440 and the Center for Ubiquitous Connectivity (CUBIC) under the JUMP 2.0 program.

average values of the FSCL decoders for polar and PAC codes when the rate profile is based on the polar code. For other rate profiles, the estimation is close to the sample average. Other special nodes in the polarization tree include repetition (REP) nodes and single parity-check (SPC) nodes [14]. For REP nodes, all the leaf nodes are frozen bits except the last one, while for SPC nodes, all the leaf nodes are information bits except the first one. In this paper, we consider all these special nodes. Furthermore, we also consider Type-I nodes [15], where all the corresponding leaf nodes are frozen bits except the last two, which are information bits. While numerous other node types in the literature can reduce complexity and latency, they often necessitate larger memory or greater computational complexity. Our method is compatible with these alternative node types as well.

Another major bottleneck in the implementation of FSCL decoding is the need to sort at each level of the polarization tree when the number of bifurcated paths exceeds L , in order to identify the best L paths. To achieve ultra-reliable performance, a larger list size may be necessary, but avoiding sorting operations can improve both latency and computational complexity. As mentioned earlier, we demonstrate that at each level of the polarization tree, the average value of our proposed optimal metric function corresponds to the polarized mutual information for the correctly decoded branch and is negative for the incorrect branch. Utilizing our proposed metric function polarization and the average metric values obtained at each level of the polarization tree, we introduce a technique to prune paths from $2L$ that diverge from these average values. This approach enables us to avoid sorting operations at many decoding levels for FSCL decoding, thereby enhancing decoding latency. For instance, for a high-rate PAC(128, 99) code constructed using the Reed-Muller rate profile, SCL decoding with a list of size 32 delivers error correction performance on par with that of the Fano algorithm. In comparison, FSCL decoding only needs to visit 28 nodes of the polarization tree, a substantial reduction from the 254 nodes needed for conventional SCL decoding. Furthermore, our approach cuts the number of sorting operations of FSCL algorithm to about 33% of the previous requirement, which further enhances latency performance at a high E_b/N_0 regime. For a PAC(1024, 512) code constructed using the polar rate profile, the reduction in sorting operations for the FSCL algorithm is even more substantial, decreasing to about 5% of the previous requirement.

The remainder of this paper is organized as follows. Sections II-B, and II-C provide brief overviews of polar codes, RM codes, and PAC codes, respectively. In Section III, we introduce the concept of metric polarization to derive an optimal metric function for each level of the polarization tree. Section IV presents the proposed average metric function for FSCL decoding and compares it with sample average metric function values across different code rates and lengths. Section V offers simulation results. Finally, Section VI concludes the paper.

II. PRELIMINARIES

A. Notation Convention

Vectors and matrices are represented in this paper by bold-face letters. All operations are performed in the binary field \mathbb{F}_2 . For a vector $\mathbf{u} = (u_1, u_2, \dots, u_N)$, subvectors (u_1, \dots, u_i) and (u_i, \dots, u_j) are denoted by \mathbf{u}^i and \mathbf{u}_i^j , respectively. For a given set \mathcal{A} , the subvector $\mathbf{u}_{\mathcal{A}}$ includes all elements u_i where i belongs to the set \mathcal{A} .

B. Polar and Reed-Muller Codes

A binary input discrete memoryless channel (BI-DMC) with an arbitrary output alphabet \mathcal{Y} is denoted by $W : \mathcal{X} \rightarrow \mathcal{Y}$. $W(y|x)$ represents the probability of a channel transition, where $x \in \mathcal{X} = \{0, 1\}$ and $y \in \mathcal{Y}$. By selecting a certain subset of the rows of $\mathbf{F}_N \triangleq \mathbf{F}^{\otimes n}$, which is the n th Kronecker power of $\mathbf{F} = \begin{bmatrix} 1 & 0 \\ 0 & 1 \end{bmatrix}$ with $n = \log_2 N$, the generator matrix of polar codes is obtained. Such a process for selection of a submatrix of \mathbf{F}_N , referred to as the rate profiling problem of polar codes, involves identifying a set \mathcal{A} to embed the information (data) bits in the data carrier vector.

The information vector \mathbf{d}^K of length K can be inserted into the vector \mathbf{u}^N as $\mathbf{u}_{\mathcal{A}} = \mathbf{d}^K$ and $\mathbf{u}_{\mathcal{A}^c} = \mathbf{0}$ for an (N, K, \mathcal{A}) polar code with $N = 2^n$, where $\mathcal{A} \subseteq \{1, 2, \dots, N\}$ corresponds to the rate profile of the code. For symmetric channels, the frozen bits $\mathbf{u}_{\mathcal{A}^c}$ are assigned to all zeros, where the complementary set \mathcal{A}^c denotes the frozen bit set. Then, the encoding is performed as $\mathbf{x}^N = \mathbf{u}^N \mathbf{F}_N$.

As a well-studied family of linear block codes, Reed-Muller (RM) codes benefit from their specific and universal construction (i.e., not channel dependent), favorable weight spectrum, and appealing structural properties [16], [17]. RM codes can be also viewed as codes in the general family of polar codes. More specifically, an $\text{RM}(r, m)$ code, with length $N = 2^m$ and dimension $K = \binom{m}{0} + \binom{m}{1} + \dots + \binom{m}{r}$, where $\binom{m}{t}$ is a binomial coefficient, can be constructed by selecting all K rows of the matrix \mathbf{F}_N that have Hamming weights greater than or equal to 2^{m-r} . The selection of row indices is a key distinction between RM codes and that of polar codes driven by their successive cancellation (SC)-type decoders. Additionally, the code dimension K in an RM code can take on $m + 1$ distinct values, whereas in polar codes K can be arbitrarily set as long as $1 \leq K \leq N$. In this paper, we use the notation $\text{RM}(N, K)$ instead of the more conventional $\text{RM}(r, m)$ notation.

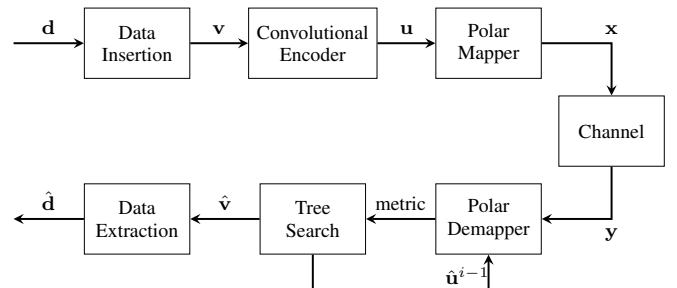


Fig. 1. Flowchart of PAC coding scheme.

C. PAC Coding Scheme

For an $(N, K, \mathcal{A}, \mathbf{T})$ PAC code, Fig. 1 illustrates a block diagram of the PAC coding scheme. Here, N and K represent the code length and data length, respectively. The set \mathcal{A} defines the code rate profile, and \mathbf{T} is a rate-one convolutional code generator matrix. More specifically, it is an upper-triangular Toeplitz matrix obtained from a connection polynomial $\mathbf{p}(x) = p_m x^m + \dots + p_1 x + p_0$, where $p_0 = p_m = 1$, and is given by

$$\mathbf{T} = \begin{bmatrix} p_0 & p_1 & p_2 & \cdots & p_m & 0 & \cdots & 0 \\ 0 & p_0 & p_1 & p_2 & \cdots & p_m & & \vdots \\ 0 & 0 & p_0 & p_1 & \ddots & \cdots & p_m & \vdots \\ \vdots & 0 & \ddots & \ddots & \ddots & \ddots & & \vdots \\ \vdots & & \ddots & \ddots & \ddots & \ddots & \ddots & \vdots \\ \vdots & & & \ddots & 0 & p_0 & p_1 & p_2 \\ \vdots & & & & 0 & 0 & p_0 & p_1 \\ \vdots & \cdots & \cdots & \cdots & \cdots & 0 & 0 & p_0 \end{bmatrix}.$$

In this paper, we use the connection polynomial $\mathbf{p}(x) = x^{10} + x^9 + x^7 + x^3 + 1$ for our simulations.

Same as in polar codes, the source vector \mathbf{d}^K is assumed to be randomly generated from a uniform distribution over $\{0, 1\}^K$. The data insertion block, based on the rate profile \mathcal{A} , converts these K bits into a data carrier vector \mathbf{v}^N , establishing a code rate $R = K/N$ ($\mathbf{v}_{\mathcal{A}} = \mathbf{d}^K$ and $\mathbf{v}_{\mathcal{A}^c} = \mathbf{0}$). Subsequently, the convolutional encoder from \mathbf{v}^N generates $\mathbf{u}^N = \mathbf{v}^N \mathbf{T}$. This step imposes a constraint on each element u_j in \mathbf{u}^N , dependent on at most m prior bits. The polar mapper then encodes \mathbf{u}^N into $\mathbf{x}^N = \mathbf{u}^N \mathbf{F}_N$. During decoding, the SCL decoder estimates \hat{v}_i . Finally, the decoded data $\hat{\mathbf{v}}^N$ allows extraction of the K -bit information based on \mathcal{A} . Instead of an SCL decoder, other tree search algorithms can also be used.

D. FSC, FSCL and Metric Functions

Fano, successive cancellation (SC) and successive cancellation list (SCL) decoding of polar and PAC codes involve traversing a polarization tree, corresponding to the channel polarization process, which is a complete tree of depth $n = \log_2(N)$ for a polar or PAC code of length N . This tree has N leaf nodes, and these conventional decoders estimate the transmitted data bits by traversing the entire tree and examining the leaf nodes. However, if all the leaf nodes of an intermediate node in the polarization tree are frozen bits (known as a rate-0 node), there is no need to traverse the corresponding subtree, as the values of the frozen bits are already known to the decoder. The same thing happens when all the leaf nodes of an intermediate node are information bits (known as a rate-1 node). Pruning the polarization tree by eliminating the need to visit the sub-trees corresponding to rate-1 and rate-0 nodes can significantly reduce the complexity and latency of decoders [12]. This advantage becomes even more evident for low-rate (with many rate-0 nodes) or high-rate (with many rate-1 nodes) polar codes. The decoders

resulting from pruning the polarization tree are referred to as fast SC (FSC) or fast SCL (FSCL) decoders. The channel polarization process can also be adjusted to account for rate-0 and rate-1 nodes [13]. Also, fast SCL and Fano decoders, which are employed in the decoding of PAC codes [18]–[20], do not often visit the last level (and may visit only up to the one before last) of the polarization tree.

The implementation of fast decoders necessitates calculating the metric function optimally at the intermediate levels of the polarization tree. In [21], the metric function used in the conventional SCL decoding algorithm is analyzed. In [22], assuming a Gaussian distribution, an ad-hoc method is proposed to avoid splitting on reliable bits by defining a threshold on the reliability of an information bit. In [23], the average of the log-likelihood ratios (LLRs) are empirically obtained, and based on that, they avoid splitting. They generalize the REP and Type-I nodes to any intermediate node with one or two information bits. This approach requires additional memory and computation to partially encode the related chunk of leaf nodes. In the rate profiles studied in this paper, we only see the information bit positions at the end of the chunk, although our method can be generalized in a straightforward fashion as well.

III. METRIC POLARIZATION

Let W^N represents N independent and identically distributed (i.i.d.) copies of the channel W . Let \mathbf{x}^N denote the length- N input to W^N and \mathbf{y}^N denote the length- N output in an uncoded system. Consider a decoder that aims to estimate the inputs of channel W^N by using the channel output values \mathbf{y}^N . Then the optimal approach, in terms of minimizing error probability, is to find the x_i values that maximize

$$p(x_i|y_i) \quad (1)$$

known as the maximum a posteriori (MAP) rule. Using Bayes' rule, this can be expressed as

$$p(x_i|y_i) = \frac{p(y_i|x_i)}{p(y_i)} p(x_i), \quad (2)$$

where $p(y_i|x_i)$ is the channel transition probability, $p(y_i)$ is the channel output probability, and $p(x_i)$ is the channel input probability.

In the absence of prior knowledge about the input distribution, or when there is no coding, one may assume a uniform distribution for the x_i values. Thus, the MAP rule simplifies to maximizing the metric function

$$\phi(x_i; y_i) \triangleq \log_2 \left(\frac{p(y_i|x_i)}{p(y_i)} \right). \quad (3)$$

This metric function can be expressed in terms of the channel log-likelihood ratio (LLR) values as

$$\begin{aligned}\phi(x_i; y_i) &= \log_2 \left(\frac{p(y_i|x_i)}{p(y_i)} \right) \\ &= \log_2 \left(\frac{p(y_i|x_i)}{\frac{1}{2} [p(y_i|x_i) + p(y_i|x_i \oplus 1)]} \right) \\ &= 1 - \log_2 \left(1 + \frac{p(y_i|x_i \oplus 1)}{p(y_i|x_i)} \right) \\ &= 1 - \log_2 \left(1 + 2^{-\log_2 \left(\frac{p(y_i|x_i \oplus 1)}{p(y_i|x_i)} \right)} \right) \\ &= 1 - \log_2 \left(1 + 2^{-L_{\text{ch}_i} \cdot (-1)^{x_i}} \right),\end{aligned}\quad (4)$$

where

$$L_{\text{ch}_i} = \log_2 \frac{p(y_i|x_i = 0)}{p(y_i|x_i = 1)} \quad (5)$$

and for a binary input additive white Gaussian noise (BI-AWGN) channel, this is equal to $\frac{2y_i}{\sigma^2}$.

In this trivial decoding algorithm for the uncoded case, the metric function determines the direction (whether x_i is zero or one) to be chosen through the code tree. This metric function should have well-diverged values for the correct and incorrect values of x_i . One way to analyze this problem is by considering the ensemble of input-output random pairs (X_i, Y_i) and evaluating the average of the metric function. The expectation of the metric can be obtained as

$$\begin{aligned}\mathbb{E}_{X_i, Y_i} [\phi(X_i; Y_i)] &= \sum_{x_i} p(x_i) \sum_{y_i} p(y_i|x_i) \phi(x_i; y_i) \\ &= \sum_{x_i} p(x_i) \sum_{y_i} p(y_i|x_i) \log_2 \left(\frac{p(y_i|x_i)}{p(y_i)} \right) \\ &= I(W),\end{aligned}\quad (6)$$

where $I(W)$ is the symmetric capacity, representing the highest achievable rate when the input x_i values have equal probabilities. Assuming that $\tilde{x}_i = x_i \oplus 1$, we have

$$\mathbb{E}_{X_i, Y_i} [\phi(\tilde{X}_i; Y_i)] \leq 0. \quad (7)$$

In the *high-capacity* regime, i.e., when the channel W is reliable, $\mathbb{E}_{X_i, Y_i} [\phi(X_i; Y_i)] = I(W)$ is close to 1. Given that the average of the metric function on the incorrect input bit is less than or equal to 0 (and in the perfect noiseless channel $\phi(\tilde{x}_i; y_i) = -\infty$), we conclude that in a relatively good channel, the soft value of this metric can effectively distinguish between the correct and incorrect values of the channel input.

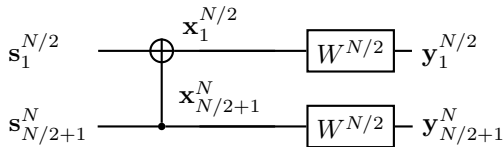


Fig. 2. Flowchart of a one-step polarization scheme.

Fig. 2 shows the one-step polarization process, which generates $N/2$ i.i.d. bad channels named W^- and $N/2$ i.i.d. good

channels named W^+ from N copies of an i.i.d. channel W . The input to the i -th bad channel is s_i , and its output is the pair $(y_i, y_{N/2+i})$. The input to the i -th good channel is $s_{N/2+i}$, and assuming that a genie correctly provides the value of s_i for the i -th bad channel, the output of the i -th good channel is $(y_i, y_{N/2+i}, s_i)$.

For the i -th bad channel, an optimal decoder should maximize

$$P(s_i|y_i, y_{N/2+i}). \quad (8)$$

Assuming a uniform distribution for its input s_i , by using Bayes' rule, an optimal decoder should maximize the value of the metric function

$$\phi^-(s_i; y_i, y_{N/2+i}) \triangleq \log_2 \left(\frac{P(y_i, y_{N/2+i}|s_i)}{P(y_i, y_{N/2+i})} \right). \quad (9)$$

After a few steps of operation, we obtain

$$\phi^-(s_i; y_i, y_{N/2+i}) = 1 - \log_2 \left(1 + 2^{-L_i \cdot (-1)^{s_i}} \right), \quad (10)$$

where

$$L_i = \log_2 \left(\frac{P(y_i, y_{N/2+i} | s_i = 0)}{P(y_i, y_{N/2+i} | s_i = 1)} \right). \quad (11)$$

For the i -th good channel, similarly, an optimal decoder should maximize

$$\begin{aligned}\phi^+(s_{N/2+i}; y_i, y_{N/2+i}, s_i) \\ \triangleq \log_2 \left(\frac{P(y_i, y_{N/2+i}, s_i | s_{N/2+i})}{P(y_i, y_{N/2+i})} \right).\end{aligned}\quad (12)$$

By considering the ensemble of input-output random pairs $(S_i; Y_i, Y_{N/2+i})$ for the i -th bad channel, the average of the corresponding metric is

$$\begin{aligned}\mathbb{E}_{S_i, (Y_i, Y_{N/2+i})} [\phi^-(S_i; Y_i, Y_{N/2+i})] \\ &= \sum_{s_i} p(s_i) \sum_{(y_i, y_{N/2+i})} P(y_i, y_{N/2+i} | s_i) \phi^-(s_i; y_i, y_{N/2+i}) \\ &= \sum_{s_i} \sum_{(Y_i, Y_{N/2+i})} p(s_i) P(y_i, y_{N/2+i} | s_i) \\ &\quad \times \log_2 \left(\frac{P(y_i, y_{N/2+i} | s_i)}{P(y_i, y_{N/2+i})} \right) = I(W^-).\end{aligned}\quad (13)$$

Assuming that $\tilde{s}_i = s_i \oplus 1$, we can also show that

$$\mathbb{E}_{S_i, (Y_i, Y_{N/2+i})} [\phi^-(\tilde{S}_i; Y_i, Y_{N/2+i})] \leq 0. \quad (14)$$

Similarly, for the i -th good channel W^+ , the average of its metric function is

$$\mathbb{E} [\phi^+(s_{N/2+i}; Y_i, Y_{N/2+i}, S_i)] = I(W^+), \quad (15)$$

and for $\tilde{s}_{N/2+i} = s_{N/2+i} \oplus 1$,

$$\mathbb{E} [\phi^+(\tilde{S}_{N/2+i}; Y_i, Y_{N/2+i}, S_i)] \leq 0. \quad (16)$$

Continuing with the recursive process, Fig. 3 illustrates the two-step polarization. The metric function ϕ^{--} corresponding to channel W^{--} is defined as

$$\begin{aligned}\phi^{--}(v_i; y_i, y_{N/4+i}, y_{N/2+i}, y_{3N/4+i}) \\ \triangleq \log_2 \left(\frac{P(y_i, y_{N/4+i}, y_{N/2+i}, y_{3N/4+i} | v_i)}{P(y_i, y_{N/4+i}, y_{N/2+i}, y_{3N/4+i})} \right).\end{aligned}\quad (17)$$

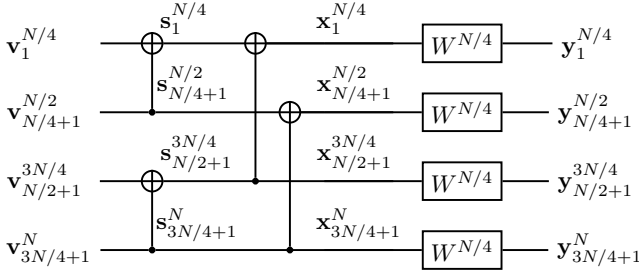


Fig. 3. Flowchart of a two-step polarization scheme.

Similarly, for channels W^{-+} , W^{+-} , and W^{++} , we define the metric functions ϕ^{-+} , ϕ^{+-} , and ϕ^{++} . Assuming the inputs of the synthesized channels are uniformly distributed, an optimal decoder should maximize the value of these metric functions.

In the same way, we can show that these optimal metric functions are equal to the corresponding channel capacities of the four synthesized channels when considering the correct input bit, and they have a negative value when the input bit is incorrect.

Continuing this process provides the polarization of the metric function on the polarization tree and is obtained by the LLRs at the corresponding depth of the tree. Assuming the input to the synthesized channel is uniform, maximizing the polarized metric functions results in an optimal decoder that can partially explore the polarization tree, similar to FSCL decoders.

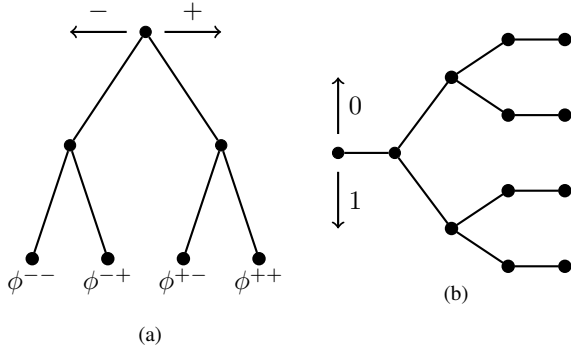


Fig. 4. (a) Polarization and (b) code tree of a PAC(4, 2) code.

Fig. 4 illustrates the polarization tree and code tree corresponding to a PAC(4, 2) code, where $\mathcal{A} = \{2, 3\}$. For K data bits, the code tree contains 2^K distinct paths from the root to each of the leaf nodes. The decoder's task is to identify the path that corresponds to the transmitted data. This involves determining whether to proceed up (corresponding to data bit 0) or down (corresponding to data bit 1). The polarization tree has at most $\log_2(N)$ levels. Using the polarization tree, the decoder computes the bit metric function values and subsequently traverses the code tree. Each leaf node of the polarization tree corresponds to a specific level of the code tree. For a Fast SCL decoder, it is not necessary to traverse the polarization tree up to the leaf level to determine the correct branch in the code tree. The following proposition characterizes the polarization of the metric function. As discussed in

[24, p. 206], we employ the standard ensemble of random linear codes for convolutional codes to conduct our analysis. This ensemble can be represented by the pair (\mathbf{T}, \mathbf{c}) in the form $\mathbf{v}\mathbf{T} + \mathbf{c}$, where \mathbf{c} is an arbitrary, fixed binary vector of length N .

We can now present the general result. Consider a convolutional code with output $\mathbf{r} = \mathbf{v}\mathbf{T} + \mathbf{c}$, where the polar mapper undergoes k steps of polarization. Define

$${}_i\mathbf{r} \triangleq (r_i, r_{N/2^k+i}, \dots, r_{(2^k-1)N/2^k+i})$$

and its corresponding channel output as

$${}_i\mathbf{y} \triangleq (y_i, y_{N/2^k+i}, \dots, y_{(2^k-1)N/2^k+i})$$

for i ranging from 1 to $N/2^k$. By employing k steps of polarization, we have 2^k of $N/2^k$ i.i.d. channels $W^{\{-,+\}^k}({}_i r_j; {}_i \mathbf{y}, {}_i \mathbf{r}_1^{j-1})$ from the original N i.i.d. channels W . Assume the decoder has obtained ${}_i \mathbf{r}_1^{j-1}$.

Proposition 1. *The optimal metric function for decoding ${}_i r_j$ is*

$$\phi^{\{-,+\}^k}({}_i r_j; {}_i \mathbf{y}, {}_i \mathbf{r}_1^{j-1}) \triangleq \log_2 \left(\frac{P({}_i \mathbf{y}, {}_i \mathbf{r}_1^{j-1} | {}_i r_j)}{P({}_i \mathbf{y}, {}_i \mathbf{r}_1^{j-1})} \right), \quad (18)$$

where i ranges from 1 to $N/2^k$, corresponding to the i -th channel of $W^{\{-,+\}^k}({}_i r_j; {}_i \mathbf{y}, {}_i \mathbf{r}_1^{j-1})$. The average value of this metric function for the correct branch is $I(W^{\{-,+\}^k}({}_i r_j; {}_i \mathbf{y}, {}_i \mathbf{r}_1^{j-1}))$, while for the incorrect branch, it is less than or equal to zero.

Proof: By the MAP rule, an optimal decoder seeks to maximize $P({}_i r_j | {}_i \mathbf{y}, {}_i \mathbf{r}_1^{j-1})$. Utilizing Bayes' rule, this can be expressed as

$$P({}_i r_j | {}_i \mathbf{y}, {}_i \mathbf{r}_1^{j-1}) = \frac{P({}_i \mathbf{y}, {}_i \mathbf{r}_1^{j-1} | {}_i r_j) P({}_i r_j)}{P({}_i \mathbf{y}, {}_i \mathbf{r}_1^{j-1})}.$$

Applying the monotonically increasing \log_2 function and assuming uniform distribution on the input of the synthesized channel, the MAP rule leads to maximizing

$$\phi^{\{-,+\}^k}({}_i r_j; {}_i \mathbf{y}, {}_i \mathbf{r}_1^{j-1}) \triangleq \log_2 \left(\frac{P({}_i \mathbf{y}, {}_i \mathbf{r}_1^{j-1} | {}_i r_j)}{P({}_i \mathbf{y}, {}_i \mathbf{r}_1^{j-1})} \right). \quad (19)$$

Considering the ensemble of input-output random pairs $({}_i R_j; {}_i \mathbf{Y}, {}_i \mathbf{R}_1^{j-1})$, the average value of the corresponding metric is

$$\begin{aligned} & \mathbb{E}_{{}_i R_j, ({}_i \mathbf{Y}, {}_i \mathbf{R}_1^{j-1})} \left[\phi^{\{-,+\}^k}({}_i R_j; {}_i \mathbf{Y}, {}_i \mathbf{R}_1^{j-1}) \right] \\ &= \sum_{{}_i r_j} P({}_i r_j) \sum_{({}_i \mathbf{y}, {}_i \mathbf{r}_1^{j-1})} P({}_i \mathbf{y}, {}_i \mathbf{r}_1^{j-1} | {}_i r_j) \\ & \quad \times \phi^{\{-,+\}^k}({}_i r_j; {}_i \mathbf{y}, {}_i \mathbf{r}_1^{j-1}) \\ &= \sum_{{}_i r_j} \sum_{({}_i \mathbf{y}, {}_i \mathbf{r}_1^{j-1})} P({}_i r_j) P({}_i \mathbf{y}, {}_i \mathbf{r}_1^{j-1} | {}_i r_j) \\ & \quad \times \log_2 \left(\frac{P({}_i \mathbf{y}, {}_i \mathbf{r}_1^{j-1} | {}_i r_j)}{P({}_i \mathbf{y}, {}_i \mathbf{r}_1^{j-1})} \right) \\ &= I \left(W^{\{-,+\}^k}({}_i r_j; {}_i \mathbf{y}, {}_i \mathbf{r}_1^{j-1}) \right). \end{aligned} \quad (20)$$

Assuming that ${}_i\tilde{r}_j = {}_i r_j \oplus 1$, we have

$$\begin{aligned}
& \mathbb{E}_{{}_i R_j, {}_i \tilde{R}_j, ({}_i \mathbf{Y}, {}_i \mathbf{R}_1^{j-1})} \left[\phi^{\{-,+\}^k} ({}_i \tilde{R}_j; {}_i \mathbf{Y}, {}_i \mathbf{R}_1^{j-1}) \right] \\
&= \sum_{{}_i \tilde{r}_j} q({}_i \tilde{r}_j) \sum_{{}_i r_j} q({}_i r_j) \sum_{({}_i \mathbf{Y}, {}_i \mathbf{R}_1^{j-1})} P({}_i \mathbf{Y}, {}_i \mathbf{R}_1^{j-1} | {}_i r_j) \\
&\quad \times \phi^{\{-,+\}^k} ({}_i \tilde{R}_j; {}_i \mathbf{Y}, {}_i \mathbf{R}_1^{j-1}) \\
&= \sum_{{}_i \tilde{r}_j} \sum_{({}_i \mathbf{Y}, {}_i \mathbf{R}_1^{j-1})} q({}_i \tilde{r}_j) P({}_i \mathbf{Y}, {}_i \mathbf{R}_1^{j-1}) \log_2 \left(\frac{P({}_i \mathbf{Y}, {}_i \mathbf{R}_1^{j-1} | {}_i \tilde{r}_j)}{P({}_i \mathbf{Y}, {}_i \mathbf{R}_1^{j-1})} \right) \\
&\leq \frac{1}{\ln(2)} \sum_{{}_i \tilde{r}_j} \sum_{({}_i \mathbf{Y}, {}_i \mathbf{R}_1^{j-1})} q({}_i \tilde{r}_j) P({}_i \mathbf{Y}, {}_i \mathbf{R}_1^{j-1}) \\
&\quad \times \left[\frac{P({}_i \mathbf{Y}, {}_i \mathbf{R}_1^{j-1} | {}_i \tilde{r}_j)}{P({}_i \mathbf{Y}, {}_i \mathbf{R}_1^{j-1})} - 1 \right] = 0, \tag{21}
\end{aligned}$$

where we used $\ln(x) \leq x - 1$ for $x > 0$. ■

IV. METRIC POLARIZATION ESTIMATION

In this section, we numerically evaluate the path metrics of FSCL decoding for PAC codes across different rate profiles. For a PAC(64, 32) code operating at $E_b/N_0 = 2.5$ dB, $\mathbb{E}[\phi(X; Y)] = 0.7944$. For the Monte Carlo (MC)-based rate profile obtained in [25], Fig. 5 shows the special nodes corresponding to this code. A conventional SCL decoder would need to visit $2N - 2 = 126$ nodes of the polarization tree. However, FSCL significantly reduces this requirement to only 22 node visits, resulting in more than a 5-fold decrease in the number of node visits. In this figure, we also show the corresponding average value of the polarized metric functions at each node. The leftmost leaf node of the tree is a Rate-0 node and contains 8 LLR values, leading to 8 metric functions, all of which have an average value of 0.1891. On the other hand, the rightmost leaf node shows an average metric function value of 1, indicating that these are reliable channels, and the decoder is most likely to detect the correct branch for them.

Fig. 6 shows the sample average path metric values for the FSCL decoding of the PAC(64, 32) code, based on 10^4 samples of correctly decoded codewords. This figure also includes the cumulative values of the average of our proposed polarized metric values derived from the polarization tree shown in Fig. 5. It can be observed that the proposed partially polarized average metric provides an excellent estimation of the actual sample average metric function values. This suggests that these values can be effectively used for normalizing metric function values in various practical settings as well.

Fig. 7 also demonstrates the metric variance of the PAC(64, 32) from Fig. 6 for the data bits. We observe that the variance at the data bits is nearly zero, suggesting that the average value of the metric function serves as an effective approximation.

Figures 8 and 9 show the sample averages of the path metric function values for FSCL decoding of the (1024, 512) and (128, 64) PAC codes, respectively. These codes use rate profiles obtained by Gaussian approximation. In these figures, we also plot our proposed average values. As the plots illustrate, the average values resulting from our proposed approach

provide an excellent match when the rate profile of the code is derived from the polar code construction.

Furthermore, Fig. 10 shows the sample average as well as our proposed average of the metric function for FSCL decoding of the PAC(128, 64) code, where the rate profile is obtained using RM code construction. In the next section, we plot the error-correction performance of the different codes studied and the average number of sorting operations required for the FSCL decoding of these codes using our proposed technique.

V. A LIST PRUNING STRATEGY AND NUMERICAL RESULTS

In this section, we present numerical results for the frame error rate (FER) performance of FSCL decoding for various PAC codes with different code lengths, code rates, and code constructions when a certain list pruning strategy is deployed based on the proposed metric. As demonstrated in the previous section, the path metric values closely follow the average values of our proposed metric in practice. Utilizing this, whenever splitting is required for the Rate-1 and SPC nodes, we examine the branch metric value. If it is lower than a threshold (denoted as m_T in our simulations), we discard that branch. For REP or Type-I nodes, we compare the cumulative branch metric values of the chunks at the end of the related segment (for REP nodes, we compare 2 paths; for Type-I nodes, we compare 4 paths). If these values are less than the threshold, we discard the corresponding path. This approach allows us to avoid sorting if the number of considered paths is less than the list size.

Fig. 11 compares the error-correction performance of our proposed pruning of FSCL with conventional SCL decoding for the PAC(128, 64) code using a list size of 32. The PAC code is constructed with the RM rate profile. In our proposed method, we prune branches where the corresponding metric function falls below $m_T = -10$. Table I shows the sample average number of sorting operations executed by our proposed pruning algorithm for the FSCL decoder of the PAC(128, 64) code, as plotted in Fig. 11. As this table shows, the average number of levels requiring pruning for a high E_b/N_0 value of 3.5 dB is almost half that of a low E_b/N_0 value.

Fig. 12 compares the error-correction performance of our proposed pruning of FSCL with conventional SCL decoding for the PAC(1024, 512) code using a list size of 4. The code is constructed with the Gaussian approximation rate profile at $E_b/N_0 = 2.5$ dB value. In our proposed method, we prune branches where the corresponding metric function falls below $m_T = -10$. Table II shows the sample average number of sorting operations executed by our proposed pruning algorithm for the FSCL decoder of the PAC(1024, 512) code, as plotted in Fig. 12. As this table shows, the average number of levels requiring sorting for a high E_b/N_0 value of 3 dB is about 5% of a conventional SCL decoding algorithm.

Fig. 13 compares the error-correction performance of our proposed pruning of FSCL with conventional SCL decoding for the PAC(64, 32) code using a list size of 32. The polar code is constructed with the MC rate profile at $E_b/N_0 = 5$ dB value

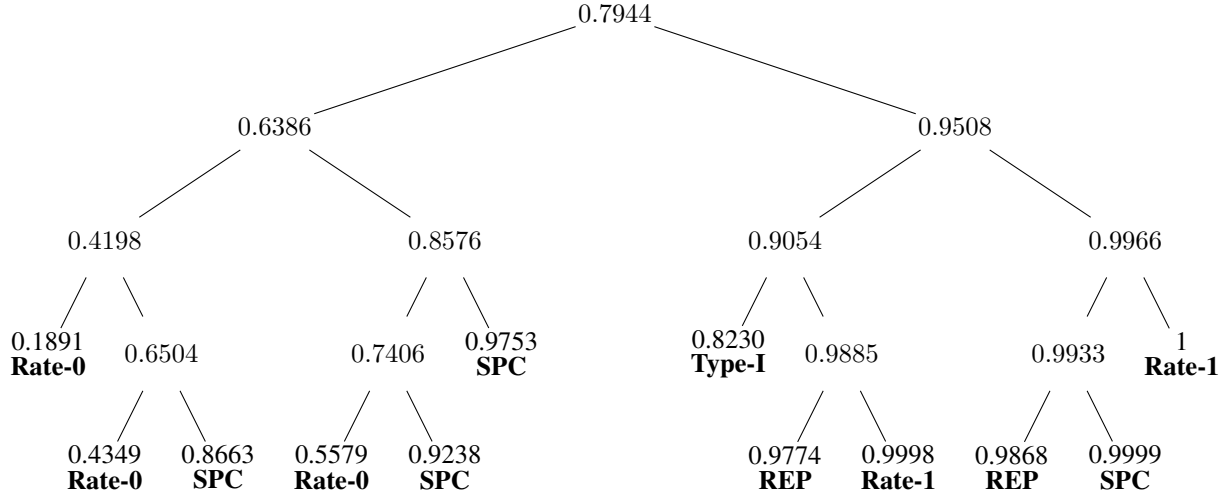


Fig. 5. Tree diagram of the average value of the partially polarized metric functions corresponding to the polarization tree of Fast SCL decoding of PAC(64, 32) code using MC rate profile.

TABLE I
SAMPLE AVERAGE NUMBER OF SORTING OPERATIONS FOR OUR PROPOSED PRUNING OF FSCL DECODER FOR THE PAC(128, 64) CODE AS PLOTTED IN FIG. 11.

E_b/N_0 [dB]	0.0	0.5	1.0	1.5	2.0	2.5	3.0	3.5
# of sorting ($L = 32, m_T = -10$)	65.93	64.53	61.79	56.60	49.89	43.04	37.29	32.78

TABLE II
SAMPLE AVERAGE NUMBER OF SORTING OPERATIONS FOR OUR PROPOSED PRUNING OF FSCL DECODER FOR THE PAC(1024, 512) CODE AS PLOTTED IN FIG. 12.

E_b/N_0 [dB]	0.0	0.5	1.0	1.5	2.0	2.5	3.0
# of sorting ($L = 4, m_T = -10$)	298.69	262.75	204.79	131.53	67.02	35.78	28.04

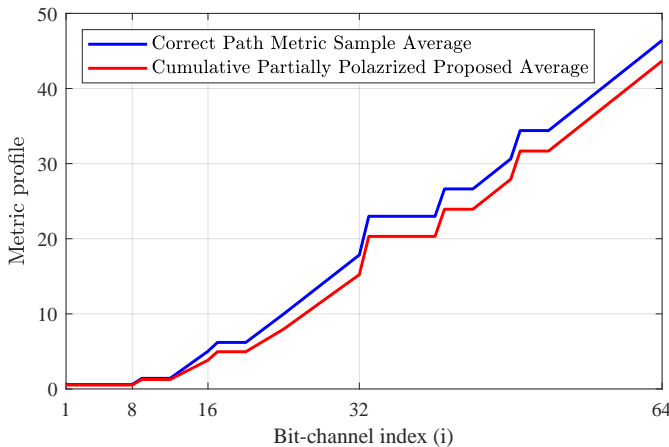


Fig. 6. Comparison of the partial optimum average path metric corresponding to the correctly decoded codewords of fast SC decoding of PAC(64, 32) code with the corresponding partially polarized channel capacity rate profile over BI-AWGN at $E_b/N_0 = 2.5$ dB with MC rate profile.

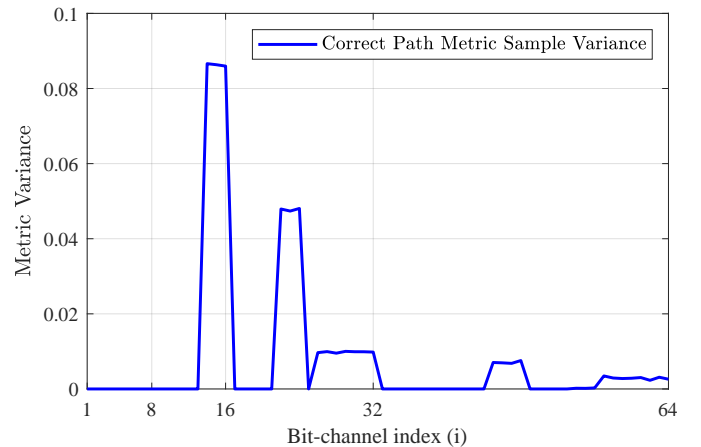


Fig. 7. Correct path metric sample variance corresponding to the correctly decoded codewords of fast SC decoding of PAC(64, 32) code of Fig. 6 over BI-AWGN at $E_b/N_0 = 2.5$ dB with MC rate profile.

[25]. In our proposed method, we prune branches where the corresponding metric function falls below $m_T = -10$. Table III shows the sample average number of sorting operations executed by our proposed pruning algorithm for the FSCL decoder of the PAC(64, 32) code, as plotted in Fig. 13.

Fig. 14 compares the error-correction performance of our proposed pruning of FSCL with conventional SCL decoding for the PAC(128, 99) code using a list size of 32. The PAC code is constructed with the RM rate profile. In our proposed method, we prune branches where the corresponding metric function falls below $m_T = -15$. Table IV shows

TABLE III
SAMPLE AVERAGE NUMBER OF SORTING OPERATIONS FOR OUR PROPOSED PRUNING OF FSCL DECODER FOR THE PAC(64, 32) CODE AS PLOTTED IN FIG. 13.

E_b/N_0 [dB]	0.0	0.5	1.0	1.5	2.0	2.5	3.0	3.5	4.0
# of sorting ($L = 32, m_T = -10$)	29.27	29.11	28.89	28.60	28.18	27.56	26.55	24.93	22.55

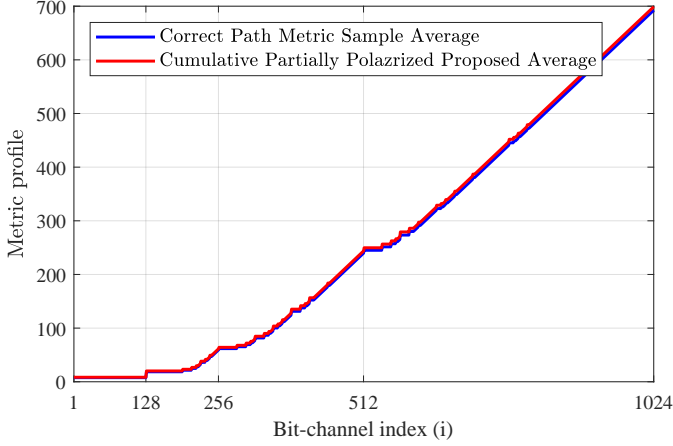


Fig. 8. Comparison of the partial optimum average path metric corresponding to the correctly decoded codewords of fast SC decoding of PAC(1024, 512) code with the corresponding partially polarized channel capacity rate profile over BI-AWGN at $E_b/N_0 = 2.5$ dB with GA rate profile.

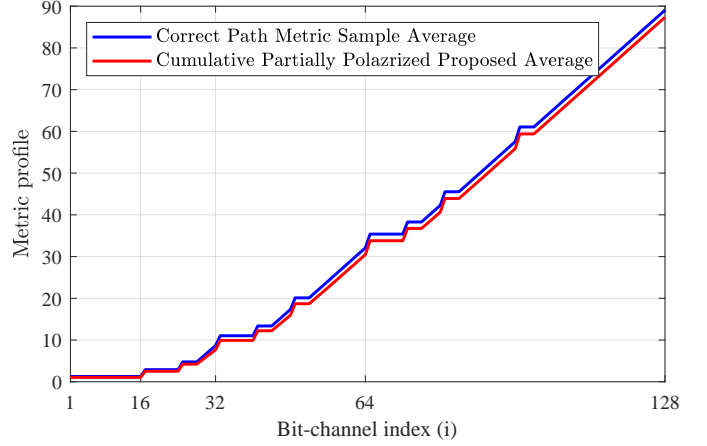


Fig. 10. Comparison of the partial average optimum path metric for correctly decoded codewords of fast SC decoding of a PAC(128, 64) code with the corresponding partially polarized channel capacity rate profile over BI-AWGN at $E_b/N_0 = 2.5$ dB, using the RM rate profile.

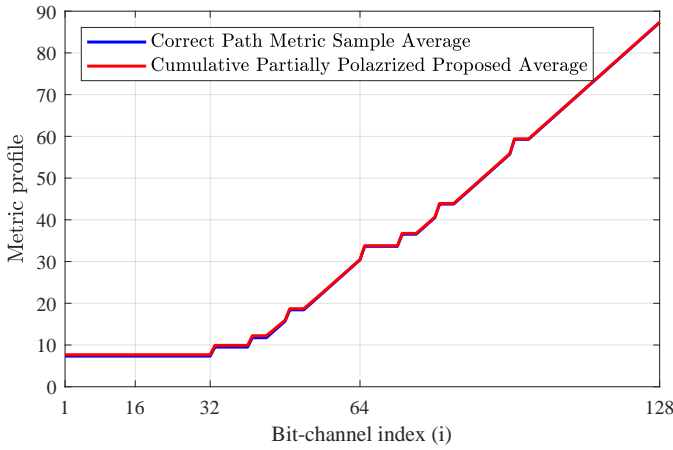


Fig. 9. Comparison of the partial optimum average path metric corresponding to the correctly decoded codewords of fast SC decoding of PAC(128, 64) code with the corresponding partially polarized channel capacity rate profile over BI-AWGN at $E_b/N_0 = 2.5$ dB with GA rate profile.

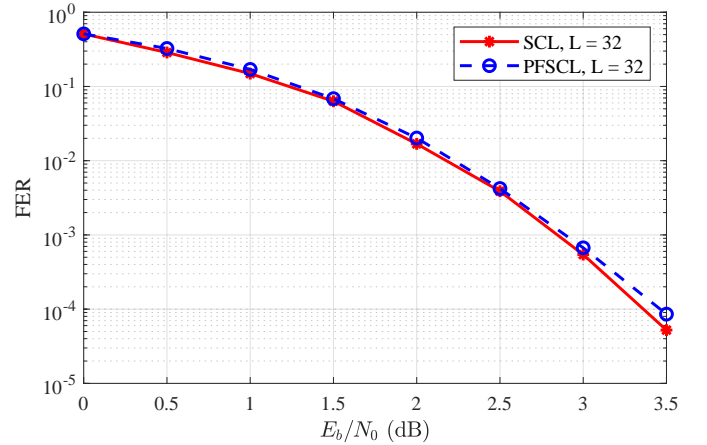


Fig. 11. Comparison of the conventional list decoding with our proposed pruning of FSCL decoding algorithm for a PAC(128, 64) code when $m_T = -10$.

the sample average number of sorting operations executed by our proposed pruning algorithm for the FSCL decoder of the PAC(128, 99) code, as plotted in Fig. 14. As this table shows, the average number of levels requiring pruning for a high E_b/N_0 value of 5 dB is about 33% of a conventional SCL decoding algorithm and the number of node visits on the polarization tree is 28 while for the conventional SCL decoding it is 254. In this figure, we have also included the FER performance of the Fano algorithm.

VI. CONCLUSION

In this paper, we introduced the concept of metric function polarization and proved that, on average, the values of the polarized metric functions are equal to the polarized mutual information. We also demonstrated that, on average, the value of the partially polarized metric function for a wrong branch is negative. By utilizing this divergence of the polarized metric functions between the correct and wrong paths, we introduced a decoding tree pruning method. This method can be used to reduce the number of sorting in FSCL algorithms that partially explore the polarization tree. Consequently, our approach can further improve the decoding latency of polar-like codes.

TABLE IV
SAMPLE AVERAGE NUMBER OF SORTING OPERATIONS FOR OUR PROPOSED PRUNING OF FSCL DECODER FOR THE PAC(128, 99) CODE AS PLOTTED IN FIG. 14.

E_b/N_0 [dB]	0.0	0.5	1.0	1.5	2.0	2.5	3.0	3.5	4.0	4.5	5
# of sorting ($L = 32, m_T = -15$)	98.31	96.50	94.77	92.93	90.32	85.28	76.44	64.45	52.76	42.66	33.43

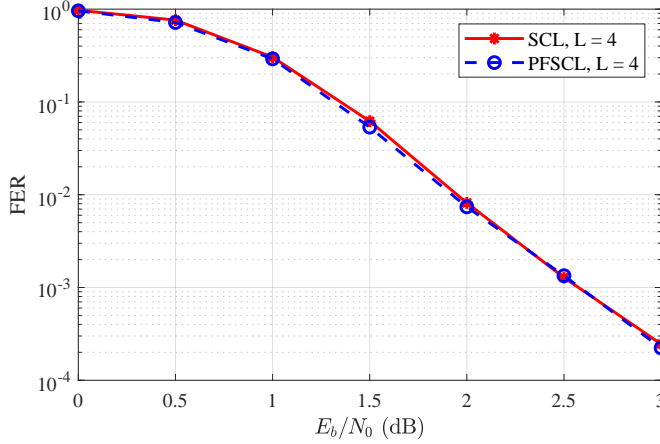


Fig. 12. Comparison of the conventional list decoding with our proposed pruning of FSCL decoding algorithm for a PAC(1024, 512) code when $m_T = -10$.

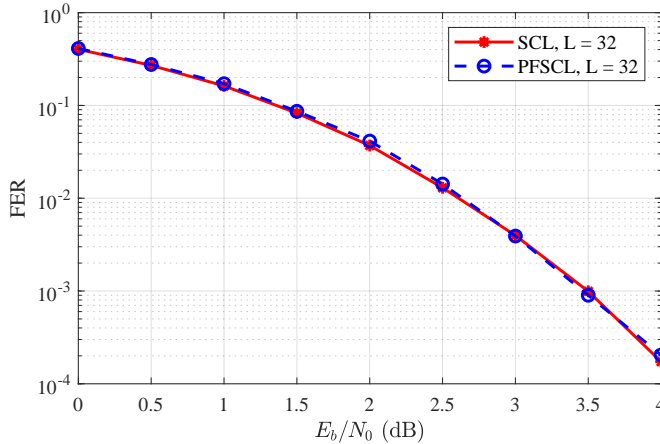


Fig. 13. Comparison of the conventional list decoding with our proposed pruning of FSCL decoding algorithm for a PAC(64, 32) code when $m_T = -10$.

REFERENCES

- [1] E. Arkan, "Channel polarization: A method for constructing capacity-achieving codes for symmetric binary-input memoryless channels," *IEEE Transactions on information Theory*, vol. 55, no. 7, pp. 3051–3073, 2009.
- [2] —, "From sequential decoding to channel polarization and back again," *arXiv preprint arXiv:1908.09594*, 2019.
- [3] M. Moradi, A. Mozammel, K. Qin, and E. Arkan, "Performance and complexity of sequential decoding of PAC codes," *arXiv preprint arXiv:2012.04990*, 2020.
- [4] B. Li, H. Zhang, and J. Gu, "On pre-transformed polar codes," *arXiv preprint arXiv:1912.06359*, 2019.
- [5] M. Moradi, "Polarization-adjusted convolutional (PAC) codes as a concatenation of inner cyclic and outer polar-and Reed-Muller-like codes," *Finite Fields and Their Applications*, vol. 93, p. 102321, 2024.
- [6] R. Fano, "A heuristic discussion of probabilistic decoding," *IEEE Transactions on Information Theory*, vol. 9, no. 2, pp. 64–74, 1963.

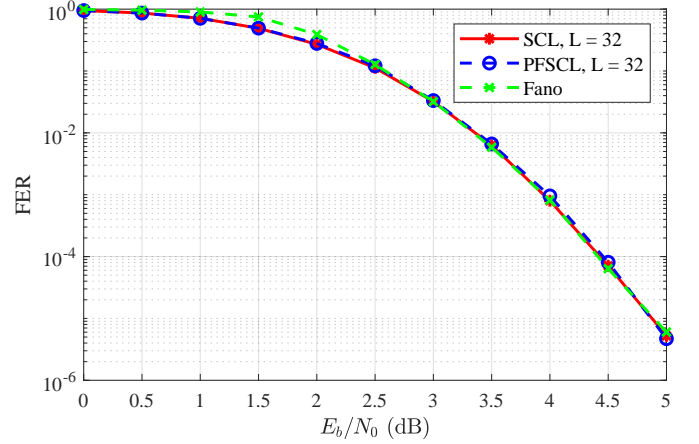


Fig. 14. Comparison of the conventional list decoding with our proposed pruning of FSCL decoding algorithm for a PAC(128, 99) code when $m_T = -15$.

- [7] M. Moradi, "On sequential decoding metric function of polarization-adjusted convolutional (PAC) codes," *IEEE Transactions on Communications*, vol. 69, no. 12, pp. 7913–7922, 2021.
- [8] —, "Application of guessing to sequential decoding of polarization-adjusted convolutional (PAC) codes," *IEEE Transactions on Communications*, vol. 71, no. 8, pp. 4425–4436, 2023.
- [9] I. Tal and A. Vardy, "List decoding of polar codes," *IEEE transactions on information theory*, vol. 61, no. 5, pp. 2213–2226, 2015.
- [10] H. Yao, A. Fazeli, and A. Vardy, "List decoding of Arkan's PAC codes," *Entropy*, vol. 23, no. 7, p. 841, 2021.
- [11] M. Rowshan, A. Burg, and E. Viterbo, "Polarization-adjusted convolutional (PAC) codes: Sequential decoding vs list decoding," *IEEE Transactions on Vehicular Technology*, vol. 70, no. 2, pp. 1434–1447, 2021.
- [12] A. Alamdar-Yazdi and F. R. Kschischang, "A simplified successive-cancellation decoder for polar codes," *IEEE communications letters*, vol. 15, no. 12, pp. 1378–1380, 2011.
- [13] M. El-Khamy, H. Mahdaviifar, G. Feygin, J. Lee, and I. Kang, "Relaxed polar codes," *IEEE Transactions on Information Theory*, vol. 63, no. 4, pp. 1986–2000, 2017.
- [14] G. Sarkis, P. Giard, A. Vardy, C. Thibeault, and W. J. Gross, "Fast polar decoders: Algorithm and implementation," *IEEE Journal on Selected Areas in Communications*, vol. 32, no. 5, pp. 946–957, 2014.
- [15] M. Hanif and M. Ardakani, "Fast successive-cancellation decoding of polar codes: Identification and decoding of new nodes," *IEEE Communications Letters*, vol. 21, no. 11, pp. 2360–2363, 2017.
- [16] D. E. Muller, "Application of Boolean algebra to switching circuit design and to error detection," *Transactions of the IRE professional group on electronic computers*, no. 3, pp. 6–12, 1954.
- [17] I. S. Reed, "A class of multiple-error-correcting codes and the decoding scheme," Massachusetts Inst of Tech Lexington Lincoln Lab, Tech. Rep., 1953.
- [18] H. Zhu, Z. Cao, Y. Zhao, D. Li, and Y. Yang, "Fast list decoders for polarization-adjusted convolutional (PAC) codes," *IET Communications*, vol. 17, no. 7, pp. 842–851, 2023.
- [19] Z.-W. Zhao, M.-M. Zhao, Y. Lu, M. Lei, and M. Li, "Fast list decoding of PAC codes with sequence repetition nodes," *IEEE Communications Letters*, 2023.
- [20] H. Ji, Y. Shen, Z. Zhang, Y. Huang, X. You, and C. Zhang, "Low-complexity fast Fano decoding for PAC codes," *IEEE Transactions on Vehicular Technology*, 2023.

- [21] M. Moradi and A. Mozammel, "A tree pruning technique for decoding complexity reduction of polar codes and PAC codes," *IEEE Transactions on Communications*, vol. 71, no. 5, pp. 2576–2586, 2023.
- [22] Z. Zhang, L. Zhang, X. Wang, C. Zhong, and H. V. Poor, "A split-reduced successive cancellation list decoder for polar codes," *IEEE Journal on Selected Areas in Communications*, vol. 34, no. 2, pp. 292–302, 2015.
- [23] X. Yao and X. Ma, "Low-complexity PSCL decoding of polar codes," *arXiv preprint arXiv:2405.13255*, 2024.
- [24] R. G. Gallager, *Information theory and reliable communication*. Springer, 1968, vol. 588.
- [25] M. Moradi and A. Mozammel, "A Monte-Carlo based construction of polarization-adjusted convolutional (PAC) codes," *arXiv preprint arXiv:2106.08118*, 2021.